UDC

T.Yu. Vergentev[1], A.G. Banshchikov [2], E.Yu. Koroleva [1,2], N.S. Sokolov [2], M.V. Zakharkin [1], N.M. Okuneva [2]

[1] St. Petersburg State Polytechnical University,
29 Politekhnicheskaya St., St. Petersburg, 195251, Russia.
[2] Ioffe Physical-Technical Institute,
26 Politekhnicheskaya St., St. Petersburg, 194021, Russia.

IN-PLANE CONDUCTIVITY OF THIN FILMS AND HETEROSTUCTURES BASED ON LaF_3-SrF_2

Т.Ю. Вергентьев, А.Г. Банщиков, Е.Ю. Королева, Н.С. Соколов, М.В. Захаркин, Н.М. Окунева

ПРОДОЛЬНАЯ ПРОВОДИМОСТЬ ТОНКИХ ПЛЕНОК И ГЕТЕРОСТРУКТУР, ОСНОВАННЫХ НА LaF_3-SrF_2

The in-plane conductivity of solid solution $La_{1-x}Sr_xF_{3-x}$ ($x = 0 \div 0.24$) films with thicknesses from 40 to 260 nm grown on glass-ceramics based on SiO_2, Al_2O_3, CaF_2 (111) and MgO (100) substrates, and LaF_3-SrF_2 heterostructures grown on MgO (100) substrates were studied by impedance spectroscopy at temperature range from room temperature to 300 °C and at frequencies from 10^{-1} to 10^6 Hz.

It was found that there was a maximum of ionic conductivity for $La_{1-x}Sr_xF_{3-x}$ ($x = 0 \div 0.24$) solid solution films at $x \approx 0.05$. The conductivity of $La_{0.95}Sr_{0.05}F_{2.95}$ films is by 2 – 4 orders of magnitude higher than that of pure lanthanum fluoride films on the substrates of magnesium oxide, sapphire and glass-ceramics. It was also shown that there was a maximum of in-plane conductivity of LaF_3-SrF_2 heterostructures for the thickness of each layer ~ 20 nm. The activation energy was evaluated from the temperature dependencies of the DC-conductivity of the films according to Arrhenius – Frenkel law. It was 400 – 800 meV for all measured samples.

SOLID SOLUTION, TYSONITE, LANTHANUM FLUORIDE, STRONTIUM FLUORIDE, IMPEDANCE, IN-PLANE CONDUCTIVITY.

Методом импедансной спектроскопии в температурном диапазоне от 300 до 570 K и частотном диапазоне от 0.1 Гц до 1 МГц, была измерена продольная проводимость тонких пленок $La_{1-x}Sr_xF_{3-x}$ ($x = 0 \div 0{,}24$) на подложках ситалла, Al_2O_3, CaF_2 (111) и MgO (100), а также продольная проводимость гетероструктур LaF_3-SrF_2 на подложках MgO (100).

ТВЕРДЫЙ РАСТВОР, ТИСОНИТ, ФТОРИД ЛАНТАНА, ФТОРИД СТРОНЦИЯ, ИМПЕДАНС, ПРОДОЛЬНАЯ ПРОВОДИМОСТЬ.

I. Introduction

During the last decades, heterostructures based on MF_2 where M = Ca, Sr, Ba, Cd, and RF_3 where R – rare-earth elements as well as solid solutions $R_{1-x}M_xF_{3-x}$ have been actively studied [1, 2]. Based on these, the prototypes of fluoride sensors [1, 2], oxygen sensors [3, 4], batteries [3] and transistors [4] have been proposed. However, there are no reports on experiments devoted to the optimization of active components of these devices.

A new approach to modification of fluoride materials was offered by Joachim Maier and co-workers [1, 2]. Creation of BaF_2-CaF_2 heterostructures with total thickness of 450 nm and different layer thicknesses (from 200 to 10 nm) resulted in increase of ionic conductivity of the samples by two orders of magnitude compared with the conductivity of pure BaF_2

and CaF_2 bulk crystals. Modeling experimental data with Guy – Chapman and Mott – Schottky's models gave good results [1, 2] which enabled the authors to suggest a mechanism of F^- ion transport to the interfaces increasing the in-plane conductivity.

The purpose of this experimental work is growing and investigating in-plane conductivity of $La_{1-x}Sr_xF_{3-x}$ solid solutions on the different types of the substrates such as glass-ceramics, Al_2O_3 and CaF_2 (111), and LaF_3-SrF_2 heterostructures on MgO (100) substrates.

II. Sample Preparation and Experimental Technique

Films of pure LaF_3, SrF_2 and solid solution $La_{1-x}Sr_xF_{3-x}$ were grown by molecular beam epitaxy (MBE) in an ultrahigh vacuum chamber, the base pressure inside being maintained below 10^{-8} Pa. Epi-ready MgO (100) substrates with the size of $10 \times 10 \times 0.5$ mm, and rectangular CaF_2(111) substrates with the sides parallel to the [1–10] and [11–2] directions were used. Single crystal CaF_2(111) substrates (8×10 mm) were prepared for growth by polishing their front side in a NH_4F water solution. Glass-ceramic based on SiO_2 and α-Al_2O_3 substrates were produced under industrial conditions. After pre-treatment with isopropyl alcohol and degreasing in the peroxide-ammonia solution, substrates were placed in the growth chamber on the front of Knudsen sells where they were heated for 20 min at 200 °C. In addition, MgO and α-Al_2O_3 substrates were then annealed to 1200 °C for 15 min. After vacuum annealing CaF_2 and glass-ceramic substrates during 10 min at 500 °C, a 200 nm buffer layer of CaF_2 was deposited at 400–800 °C on the polished side of CaF_2 substrates to smooth the surface. Ca, La and Sr fluorides were grown by evaporation of the materials in amorphous carbon crucibles. The growth chamber was equipped with a Reflection High Energy Electron Diffraction (RHEED) diffractometer for *in situ* characterization of the substrate surface prior to the growth and for monitoring the growing films. The deposition rates for evaporated fluorites were 2–3 nm/min as measured with a quartz microbalance.

There were grown solid solution $La_{1-x}Sr_xF_{3-x}$ ($x = 0 \div 0.24$) films with thicknesses from 40 to 260 nm placed on glass-ceramics, α-Al_2O_3, CaF_2 (111), MgO (100) substrates and heterostructures with different quantities of alternating LaF_3-SrF_2 layers. LaF_3 layer was the first to be grown on the substrates of MgO (100) with 200 nm total thickness for all samples. According to this thickness, the total number of LaF_3 and SrF_2 layers varied from $N = 2$ to 40. Each grown heterostructure had 200 nm of thickness. For example, if the number of layers were $N = 4$, it meant that the thickness of each (LaF_3 or SrF_2) layer was 50 nm. To apply the same quantity of ionic material, the thickness of LaF_3 was the same of SrF_2 one, and the total number of layers was even.

Later on, after short exposure to air, the gold electrodes were deposited on the grown heterostructures for electrical conductivity measurements. Interdigital Electrodes (IDE) were used for measuring in-plane conductivity of the films and heterostructures. The electrophysical parameters of the layers were measured with dielectric spectrometer Novocontrol BDS'80 in the wide temperature (300 – 570 K) and frequency (10^{-1} – 10^6 Hz) ranges. The magnitude of field strength was $V_{rms} = 50$ V/cm. The relative errors of the impedance and capacity did not exceed ~ $3 \cdot 10^{-5}$. The stability of temperature was better than 0.1 K.

III. Results and Discussion

A. The Conductivity of Substrates

Figure 1 shows the electrical conductivity

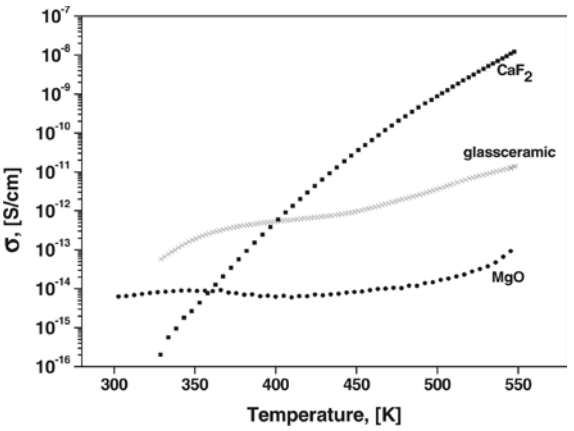

Fig. 1. Temperature dependence of the conductivity of the substrates: glass-ceramic, calcium fluoride (CaF_2) and magnesium oxide (MgO) at 0.1 Hz

behavior of CaF_2, MgO and glass-ceramic substrates, which were used in the work. Evidently, all the substrates are good dielectrics with conductivity $10^{-15} \div 10^{-11}$ S/cm in the measured temperature interval. However, the electrical conductivity of the CaF_2 substrate is strongly temperature dependent. With temperature increased by approximately 250 °C, the conductivity of CaF_2 substrate increases by 7 orders of magnitude due to calcium fluoride as an ionic conductor. Temperature behavior is well described by Arrhenius – Frenkel's law. Temperature dependences of the own conductivities of magnesium oxide and glass ceramic substrates are much smaller.

B. Comparison of the Conductivity of Thin Films Grown on the Glass-ceramic Substrates and Bulk Single Crystal

The frequency dependencies of $La_{1-x}Sr_xF_{3-x}$ thin film conductivity are shown in Fig. 2, *a*; they are typical for all examined samples. They can be divided into three regions: *1* (low frequency) – the region of conductivity increasing due to lower accumulation of charge in the electrode regions with the frequency increase, *2* (medium frequency) – frequency-independent regions and *3* (high frequency) is the universal dynamic response [1]. Analysing frequency-independent region, $\sigma(\omega)$ one can estimate the value of solid electrolyte DC-conductivity. However, such an assessment would be quite rough, more specifically DC-conductivity can be determined from the impedance hodograph (Nyquist diagram for the impedance, Fig. 2, *b*) $Z'' = f(Z')$ as

$$\sigma_{DC} = \frac{1}{R_v}\frac{d}{S},$$

where d is the distance between electrodes; S – square of the end part of heterostructure under the electrode; R_v – resistance of solid electrolytes (intersection semicircle and real part of impedance Z''). The Nyquist's plots of investigated samples consist of a semicircle and a sloped line, and this is typical for solid electrolyte systems [1].This type of the hodograph corresponds to the equivalent circuit, which consists of *RC*-chain with Warburg impedance (inset in Fig. 2, *b*) [14]. However, it characterizes the conductivity of the electro-chemical cell, which exists due to the conductivity of the film and conductivity of the substrate. The conductivity of the film can be calculated by subtracting the substrate conductivity. In our case, Kidner and co-worker's mathematical approach [15, 16] is used.

Figure 3 shows the dependence of the conductivity of $La_{1-x}Sr_xF_{3-x}$ and bulk single crystals [2]. One can see that only pure LaF_3 is a good dielectric, and even at relatively low concentrations of impurities SrF_2 ~ 1 ÷ 2 %, the conductivity of LaF_3 increases by several orders of magnitude. Both curves exhibit a

a) *b*)

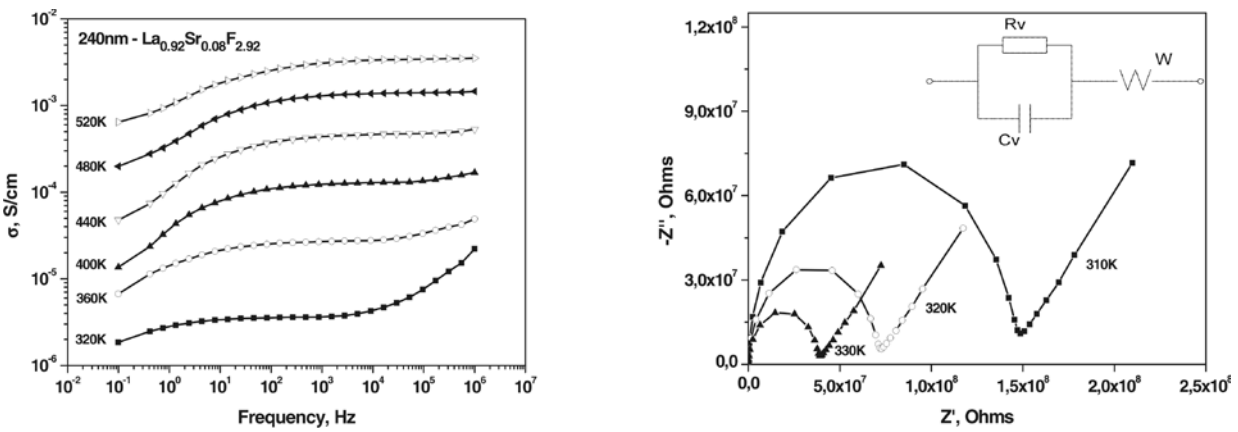

Fig. 2. *a* – Frequency dependence of the conductivity of 240 nm thick $La_{0.92}Sr_{0.08}F_{2.92}$ film at different temperatures; *b* – impedance diagrams of the same film at different temperatures.
Inset in (*b*): equivalent circuit consisting of double electric layer capacity at the interface with the electrode *Cv*, the volume resistance of the film R_v, and the Warburg element *W*

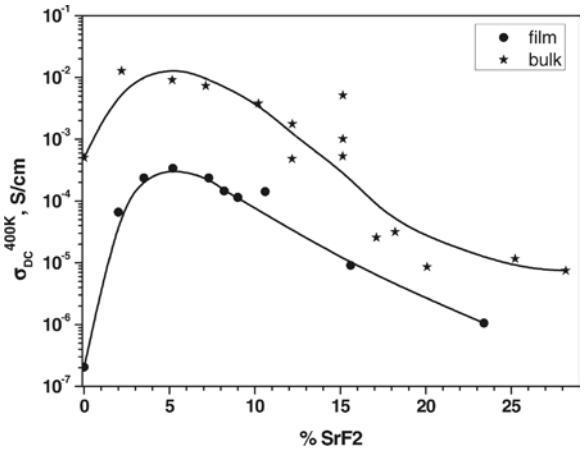

Fig. 3. Concentration dependence of the conductivity at 400 K of the $La_{1-x}Sr_xF_{3-x}$ thin films on the glass-ceramic substrates and the conductivity of bulk single crystals according to [2]

maximum of conductivity at ~ 5 % of the SrF_2 content. Conductivity of the films depending on the composition varies by four orders of magnitude, but the absolute value of the conductivity of the films is lower than the corresponding single crystal value [1, 2]. Such features can be explained by the imperfection of the crystal structure of obtained films grown at lower temperature glass-grained glass-ceramic substrates. It is not unexpected that such films show lower conductivity due to their amorphous or polycrystalline structure.

Activation energies found from the dependence of Arrhenius – Frenkel and varying from 680 meV for pure LaF_3 to 495 – 560meV for $La_{1-x}Sr_xF_{3-x}$ solid solutions, quantitatively agree with the values of activation energy of the conductivity found in [1, 2]. It should be noted that within the error bars, these values correspond to the values of the activation energy of the diffusion process obtained from the analysis of Warburg impedance at the temperatures up to 400 K. This means that the conductivity at low temperatures may be related to the diffusion mechanism [1, 2]. It is observed that the activation energy in these solid solutions strongly depends on SrF_2 content.

C. LaF_3 Thin Films on the CaF_2 and Glass-Ceramic Substrates

Epitaxial growth of $La_{1-x}Sr_xF_{3-x}$ films on CaF_2 (111) substrates is possible. However, their electric properties are different from those of the films on glass-ceramic substrates (Fig. 4). The DC-conductivity of pure LaF_3 on CaF_2 (111) substrates is higher, and it is not possible to distinguish the individual properties of the film from the substrate ones within impedance spectroscopy method. It is possible that interdiffusion of the materials leads to the formation of a solid solution in the interface of substrate and film. In this case it can be assumed that the conduction occurs along the interface and solid solution at the interface is formed. This assumption is also confirmed by the fact that the conductivity and the activation energy of conductivity for $La_{0.95}Sr_{0.05}F_{2.95}$ films on the two substrates differ a little. The highest conductivity among solid solutions based on LaF_3 has 5 % SrF_2 solid solution [2].

D. LaF_3-SrF_2 Heterostructures on MgO Substrates

The in-plane conductivity of grown heterostructures with different layer thicknesses from 100 to 5 nm are measured by impedance spectroscopy. The temperature dependencies of DC-conductivity of several grown heterostructures are shown in Fig. 5; they obey Arrhenius – Frenkel's law. The inset in this figure shows the energy activation behavior in studied samples. It is seen that the lowest activation

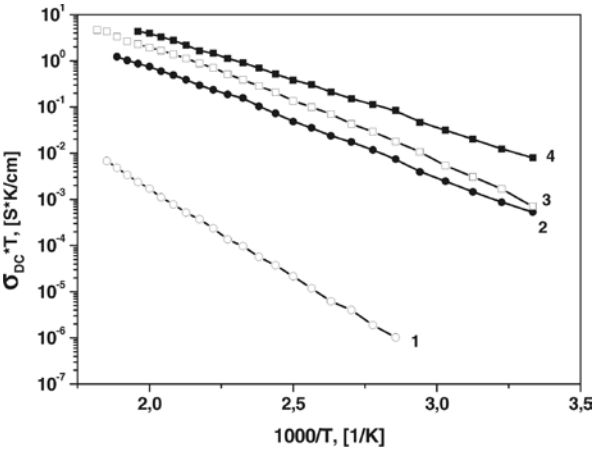

Fig. 4. *1*, *3* – DC-conductivity of thin films of pure LaF_3 and 5 % solid solution on the glass-ceramic substrates, respectively; *2*, *4* – DC-conductivity of thin films of pure LaF_3 and 5 % solid solution on the CaF_2 (111) substrates, respectively

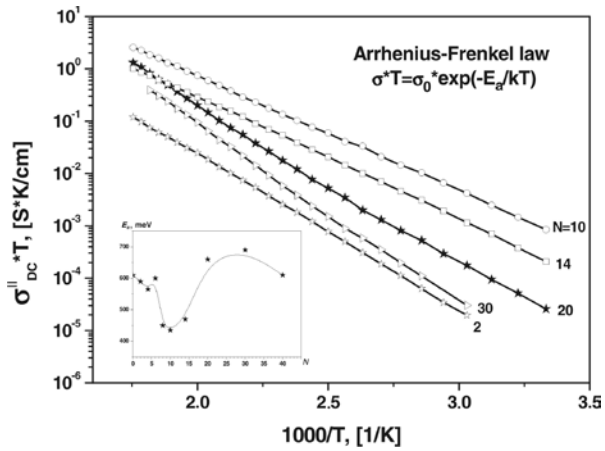

Fig. 5. Temperature behavior of the planar conductivity for several heterostructures, where N is the number of the layers.
The inset is the activation energy of the samples taken from Arrhenius – Frenkel's law

energy is demonstrated by the heterostructures with N from 6 to 10 and it equals ~430 meV. The general shape of in-plane conductivity has a peak near $N = 10$ (20 nm per layer) for all measured temperatures (Fig. 6).

For the samples with $N \geq 20$ (in which the thickness of each layer is less than 20 nm), gradual modification of the hodograph shapes is observed. Namely, the semicircle moves below the x-axis Re(Z) and the circuit can be described by equivalent circuit with CPE-element (constant phase element) and it has impedance

$$Z^*_{\mathrm{CPE}} = Z_0(j\omega)^n = \left(\frac{Z_0}{\omega^n}\right)\left[\cos\left(\frac{\pi n}{2}\right) - j\sin\left(\frac{\pi n}{2}\right)\right],$$

where $0 \leq n \leq 1$.

At $n = 0$ limit, Z^*_{CPE} does not depend on frequency and $Z_0 = R$; when $n = 1$ value Z_0 is inverse capacitance:

$$Z_0 = 1/C,$$

$$Z^*_{\mathrm{CPE}} = -\frac{1}{\omega C} \text{ [14].}$$

Thus, semicircle displacement below x-axis by an angle φ satisfies

$$\varphi = (1 - n)\ 90\ ^\circ.$$

In other words, the similar equivalent circuit broadens out of the Debay spectra and it is described by Cole – Cole spectra [3, 4]:

$$\sigma(\omega) = \sigma_\infty + \frac{\sigma_0 - \sigma_\infty}{1 + (j\omega\tau)^n}.$$

Deviation in Debay spectra for the samples $N \geq 20$ is not pronounced and $n \approx 0.85$ in the whole measured temperature range.

For comparison, Fig. 7 shows temperature behavior of planar thin film conductivity of pure LaF_3, SrF_2 and based on them $La_{1-x}Sr_xF_{3-x}$ solid solution with $x = 0.05$ and $x = 0.5$. The DC-conductivity of pure SrF_2 is estimated above 500 K only; its activation energy is 770 meV. The $La_{0.95}Sr_{0.05}F_{2.95}$ solid solution has the highest conductivity among all the possible combinations of solid solutions $LaF_3 + SrF_2$ [2], and in our case it has high conductivity with low activation energy ~420 meV. According

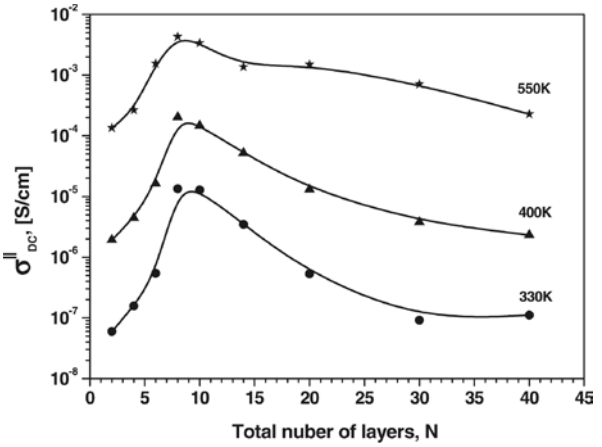

Fig. 6. Dependencies of conductivity of the heterostructures from the number of layers for different temperatures (total thickness is 200 nm)

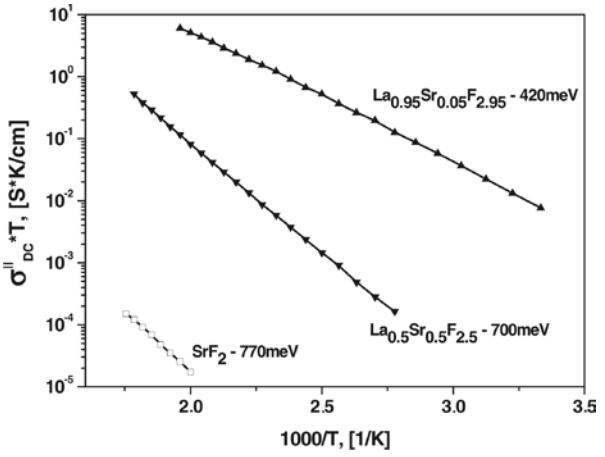

Fig. 7. The temperature behavior of the in-plane conductivity of SrF_2 films and the $La_{1-x}Sr_xF_{3-x}$ solid solutions ($x = 0.05$ and 0.5) grown on MgO (100) substrates.
The thickness of all the films is 200 nm

to [3], the 50 % solid solution of $La_{0.5}Sr_{0.5}F_{2.5}$ must have two different mixed phases: LaF_3 and defect cluster with SrF_2, separately. However, it was expected that it would be seen on the hodograph of impedance as a combination of two semicircles (two different processes of conductivity), but it is not observed in our case. RHEED does not show the characteristics associated with this fact, the diffraction patterns of the 50 % solid solution are not qualitatively different from the diffraction pattern of the 5 % solid solution.

Thus, the values of all the investigated planar DC-conductivities of the heterostructures are in the range of the conductivities of pure LaF_3 and $La_{0.95}Sr_{0.05}F_{2.95}$ solid solution. Therefore, one can assume the existence of thin interface layers enriched by F^- ions.

IV. Conclusion

The planar conductivity of $La_{1-x}Sr_xF_{3-x}$ ($x = 0 \div 0.24$) solid solution films with thicknesses from 40 to 260 nm grown on glass-ceramics, Al_2O_3, CaF_2 (111) and MgO (100), as well as heterostructures with alternating LaF_3-SrF_2 layers and total thickness of 200 nm grown on MgO (100) substrates were studied by the method of impedance spectroscopy at the temperatures ranging from room temperature to 300 °C and at frequencies from 10^{-1} to 10^6 Hz.

The highest conductivity is observed for $La_{0.95}Sr_{0.05}F_{2.95}$ films and it is hardly depends on the type of used substrates. However, the properties of pure LaF_3 on CaF_2 (111) and other substrates studied in this work are different. It may be due to the fact that the CaF_2/LaF_3 interface consists of a layer of solid solution which has been created by diffusing both components into each other.

The highest conductivity among grown on MgO (100) heterostructures is observed for the structures with $N = 10$, which corresponds to the thickness of 20 nm per each layer. This sample with 10 ordered layers of LaF_3-SrF_2 demonstrates conductivity by one order of magnitude higher than that of 50 % solid solution. Also, deviation from Debay spectra is observed in the samples with $N > 20$, it can be the result of strong mechanical stresses in the heterostructures.

The activation energies were evaluated from the temperature dependencies of the DC-conductivities of the films according to Arrhenius – Frenkel's law. The activation energies for solid solutions are ~495 – 560 meV and ~700 meV for pure LaF_3 film. The activation energies of heterostructures have the lowest values at N from 6 to 10, and they are ~430 meV, which is comparable to the activation energy for 5 % solid solution.

Acknowledgments

The work at SPbSPU was supported by Federal Program «Research and Development on High-Priority Directions of Improvement of Russia's Scientific and Technological Complex» for the years 2007–2013, Federal Program «Scientific and scientific and pedagogical shots of innovative Russia for 2009–2013»; at the Ioffe Institute it was supported by Russian Foundation for Basic Researches (grant 13-02-12429).

REFERENCES

1. **Sorokin N.I., Fominykh M.V., Krivandina E.A., Zhmurova Z.I., Sobolev B.P.** Ion transport in $R_{1-x}Sr_xF_{3-x}$ (R = La-Yb, Y) solid solutions with a LaF_3 (tysonite) structure. *Crystallography Reports*, 1996, Vol. 41, No. 4, pp. 292–310.

2. **Sorokin N.I., Sobolev B.P.** Frequency response of the low-temperature ionic conductivity of single crystals $R_{1-y}M_yF_{3-y}$ (R = La-Er; M = Ca, Sr, Ba, Cd). *Physics of the Solid State*, 2008, Vol. 50, No.3, pp. 416–421.

3. **Moritz W., Krause S., Vasiliev A.A., Godovskiy D.Yu., Malyshev V.V.** Monitoring of HF and F_2 using a field-effect sensor. *Sensors Actuators B. Chemical*, 1995, Vol. 24–25, pp. 194–196.

4. **Fergus Jeffrey W.** The application of solid fluoride electrolytes in chemical sensors. *Sensors Actuators B Chemical*, 1997, Vol. 42, pp. 119–130.

5. **Tan G.L., Wu X.J., Wang L.R., Chen Y.Q.** Investigation for oxygen sensor of LaF_3 thin film. *Sensors Actuators B. Chemical*, 1996, Vol. 34, pp. 417–421.

6. **Katsube T., Hara M., Serizawa I., Ishibashi N., Adachi N., Miura N., Yamazoe N.** MOS-type micro-oxygen sensor using LaF_3 workable at room temperature. *Japanese Journal of Applied Physics*, 1990, Vol. 29, No. 8, pp. 1392–1395.

7. **Reddy M.A., Fichtner M.** Batteries based on fluoride shuttle. *Journal of Material Chemistry*, 2011, Vol. 21, No. 43, pp. 17009–17548.

8. **Na X., Niu W., Li H., Xie J.** A novel dissolved

oxygen sensor based on MISFET structure with Pt-LaF_3 mixture film. *Sensors Actuators B. Chemical*, 2002, Vol. 87, pp. 222–225.

9. **Sata N.**, **Eberman K., Eberl K., Maier J.** Mesoscopic fast ion conduction in nanometre-scale planar heterostructures. *Nature*, 2000, Vol. 408, pp. 946–949.

10. **Guo X.X.**, **Matei I., Lee J.-S., Maier J.** Ion conduction across nanosized CaF/BaF multilayer heterostructures. *Applied Physics Letters*, 2007, Vol. 91. p. 103102.

11. **Guo X.X., Matei I., Jamnik J., Lee J.S., Maier J.** Defect chemical modeling of mesoscopic ion conduction in nanosized CaF_2/BaF_2 multilayer heterostructures. *Physical Review B*, 2007, Vol. 76, p. 125429.

12. **Guo X.X.**, **Maier J.** Comprehensive modeling of ion conduction of nanosized CaF2/BaF2 multilayer heterostructures. *Advanced Functional Materials*, 2009, Vol. 19, pp. 96–101.

13. **Ahmad M.M.**, **Yamada K., Okuda T.** Fluoride ion diffusion of superionic PbSnF4 studied by nuclear magnetic resonance and impedance spectroscopy. *J. Phys.: Condens. Matter*, 2002, Vol. 14, p. 7233.

14. **Ivanov-Schitz A.K.**, **Murin I.V.** *Solid State Ionics*: Vol. 1. St. Petersburg, SPbSU, 2000. 617 p. (rus)

15. **Kidner N.J., Homrighaus Z.J., Mason T.O., Garboczi E.J.** Modeling interdigital electrode structures for the dielectric characterization of electroceramic thin films. *Thin Solid Films*, 2006, No. 496, pp. 539–545.

16. **Kidner N.J., Meier A., Homrighaus Z.J., Wessels B.W., Mason, T.O., Garboczi E.J.** Complex electrical (impedance/dielectric) properties of electroceramic thin films by impedance spectroscopy with interdigital electrodes. *Thin Solid Films*, 2007, No. 515, pp. 4588–4595.

17. **Sher A.**, **Solomon R., Lee K., Muller M.W.** Transport Properties of LaF_3. *Physical Review*, 1966, Vol. 144, No. 2, pp. 593–604.

18. **Wei Y.Z., Sridhar S.** A new graphical representation for dielectric data. *J. Chem. Phys*, 1993, 99(4), p. 3119.

19. **Vergent'ev T.Yu.**, **Koroleva E.Yu., Kurdyukov D.A., Naberezhnov A.A., Filimonov A.V.** Behavior of the low-frequency conductivity of silver iodide nanocomposites in the superionic phase transition region. *Physics of the Solid State*, 2013, Vol. 55, No. 1, pp. 175–180.

20. **Ivanov-Schitz A.K.**, **Sorokin N.I., Sobolev B.P., Fedorov P.P.** Ionic transport in systems MF2-RF3 (M = Ca, Sr, Ba; R = La-Ln). *Proc. Int. symp. on systems with the fast ionic transport.* Bratislava, Smolenia, 1985, p. 99–103.

СПИСОК ЛИТЕРАТУРЫ

1. **Сорокин Н.И., Фоминых М.В., Кривандина Е.А., Жмурова З.И., Соболев Б.П.** // Кристаллография. 1996. Т. 41. № 2. С. 310 – 315.

2. **Сорокин Н.И., Соболев Б.П.** Частотные зависимости ионной проводимости монокристаллов $R_{1-y}M_yF_{3-y}$ (R = La·Er, M = Ca, Sr, Ba, Cd) при низких температурах // ФТТ. 2008. Т. 50. Вып. 3. С. 402 – 407.

3. **Moritz W., Krause S., Vasiliev A.A., Godovskiy D.Yu., Malyshev V.V.** Monitoring of HF and F_2 using a field-effect sensor. *Sensors Actuators B. Chemical*, 1995, Vol. 24–25, pp. 194–196.

4. **Fergus Jeffrey W.** The application of solid fluoride electrolytes in chemical sensors. *Sensors Actuators B Chemical*, 1997, Vol. 42, pp. 119–130.

5. **Tan G.L., Wu X.J., Wang L.R., Chen Y.Q.** Investigation for oxygen sensor of LaF_3 thin film. *Sensors Actuators B. Chemical*, 1996, Vol. 34, pp. 417–421.

6. **Katsube T., Hara M., Serizawa I., Ishibashi N., Adachi N., Miura N., Yamazoe N.** MOS-type micro-oxygen sensor using LaF_3 workable at room temperature. *Japanese Journal of Applied Physics*, 1990, Vol. 29, No. 8, pp. 1392–1395.

7. **Reddy M.A., Fichtner M.** Batteries based on fluoride shuttle. *Journal of Material Chemistry*, 2011, Vol. 21, No. 43, pp. 17009–17548.

8. **Na X., Niu W., Li H., Xie J.** A novel dissolved oxygen sensor based on MISFET structure with Pt-LaF_3 mixture film. *Sensors Actuators B Chemical*, 2002, Vol. 87, pp. 222–225.

9. **Sata N.**, **Eberman K., Eberl K. & Maier J**. Mesoscopic fast ion conduction in nanometre-scale planar heterostructures. *Nature*, 2000, Vol. 408, pp. 946–949.

10. **Guo X.X.**, **Matei I., Lee J.-S., Maier J.** Ion conduction across nanosized BaF multilayer heterostructures. *Applied Physics Letters*, 2007, Vol. 91. p. 103102.

11. **Guo X.X., Matei I., Jamnik J., Lee J.S., Maier, J.** Defect chemical modeling of mesoscopic ion conduction in nanosized CaF_2/BaF_2 multilayer heterostructures. *Physical Review B*, 2007, Vol. 76, p. 125429.

12. **Guo X.X.**, **Maier J.** Comprehensive modeling of ion conduction of nanosized CaF_2/BaF_2 multilayer heterostructures. *Advanced Functional Materials*, 2009, Vol. 19, pp. 96–101.

13. **Ahmad M.M.**, **Yamada K., Okuda T.** Fluoride ion diffusion of superionic $PbSnF_4$ studied by nuclear magnetic resonance and impedance spectroscopy. *J. Phys.: Condens. Matter*, 2002,

Vol. 14, p. 7233.

14. **Иванов-Шиц А.К., Мурин И.В.** Ионика твердого тела. Т. 1. СПб.: Изд-во СПбГУ, 2000. 616 с.

15. **Kidner N.J., Homrighaus Z.J., Mason T.O., Garboczi E.J.** Modeling interdigital electrode structures for the dielectric characterization of electroceramic thin films. *Thin Solid Films*, 2006, No. 496, pp. 539–545.

16. **Kidner N.J., Meier A., Homrighaus Z.J., Wessels B.W., Mason T.O., Garboczi E.J.** Complex electrical (impedance/dielectric) properties of electroceramic thin films by impedance spectroscopy with interdigital electrodes. *Thin Solid Films*, 2007, No. 515, pp. 4588–4595.

17. **Sher A., Solomon R., Lee K., Muller M.W.** Transport properties of LaF_3. *Physical Review*, 1966, Vol. 144, No. 2, pp. 593–604.

18. **Wei Y.Z., Sridhar S.** A new graphical representation for dielectric data. *J. Chem. Phys*, 1993, Vol. 99, No. 4, p. 3119.

19. **Вергентьев Т.Ю., Королева Е.Ю., Курдюков Д.А., Набережнов А.А., Филимонов А.В.** Поведение низкочастотной проводимости нанокомпозитного иодида серебра в области суперионного фазового перехода// ФТТ. 2013. Т. 55. Вып. 1. С. 157 – 162.

20. **Ivanov-Schitz A.K., Sorokin N.I., Sobolev B.P., Fedorov P.P.** Ionic transport in systems MF_2-RF_3 (M = Ca, Sr, Ba; R=La-Ln). *Proc. Int. symp. on systems with the fast ionic transport.* Bratislava, Smolenia, 1985, p. 99–103.

ВЕРГЕНТЬЕВ Тихон Юрьевич – *аспирант кафедры физической электроники Санкт-Петербургского государственного политехнического университета.*
195251, Россия, Санкт-Петербург, Политехническая ул., 29
tikhon.v@gmail.com

БАНЩИКОВ Александр Гаврилович – *кандидат физико-математических наук, старший научный сотрудник Физико-технического института им. А.Ф. Иоффе РАН.*
194021, Россия, Санкт-Петербург, Политехническая ул., 26
aban88@bk.ru

КОРОЛЕВА Екатерина Юрьевна – *кандидат физико-математических наук, старший научный сотрудник Физико-технического института им. А.Ф. Иоффе РАН, доцент кафедры физической электроники Санкт-Петербургского государственного политехнического университета.*
194021, Россия, Санкт-Петербург, Политехническая ул., 26
e.yu.koroleva@mail.ioffe.ru

СОКОЛОВ Николай Семенович – *доктор физико-математических наук, ведущий научный сотрудник Физико-технического института им. А.Ф. Иоффе РАН.*
194021, Россия, Санкт-Петербург, Политехническая ул., 26
nsokolov@fl.ioffe.ru

ЗАХАРКИН Максим Валерьевич – *студент Института физики, нанотехнологий и телекоммуникаций Санкт-Петербургского государственного политехнического университета.*
195251, Россия, Санкт-Петербург, Политехническая ул., 29
maxim.zakh@gmail.com

ОКУНЕВА Нина Михайловна – *кандидат физико-математических наук, старший научный сотрудник Физико-технического института им. А.Ф. Иоффе РАН.*
194021, Россия, Санкт-Петербург, Политехническая ул., 26
nina.okuneva@mail.ioffe.ru